Modeling Solubility of Polycyclic Aromatic Compounds in Subcritical Water

ARTICLE *in* INDUSTRIAL & ENGINEERING CHEMISTRY RESEARCH · SEPTEMBER 2011

Impact Factor: 2.59 · DOI: 10.1021/ie201019b

2 AUTHORS, INCLUDING:

Victor Hugo Alvarez Alvarez
Camber Technology Corporation
44 PUBLICATIONS **803** CITATIONS

I&EC research
Industrial & Engineering Chemistry Research

ARTICLE

pubs.acs.org/IECR

Modeling Solubility of Polycyclic Aromatic Compounds in Subcritical Water

Víctor H. Alvarez and Marleny D. A. Saldaña*

Department of Agricultural, Food and Nutritional Science, University of Alberta, Edmonton, Alberta, Canada, T6G 2P5

Supporting Information

ABSTRACT: Polycyclic aromatic compounds (PACs) are common environmental contaminants associated with oil spills and the incomplete combustion of organic materials. PAC solubility in water is a fundamental property for environmental studies, and modeling of these data improve the process of environmental risk assessment. In this study, seven models (UNIQUAC, local surface Guggenheim, NRTL, regular solution, Wilson, Van Laar, and a modified Van Laar model) for correlations and prediction of aqueous solubilities of 22 PACs were evaluated. The results using models based on Guggenheim's method showed that the local surface Guggenheim model provided a better correlation than the UNIQUAC model. For the systems studied, the best correlations were obtained with NRTL, Van Laar, and modified Van Laar models with mean deviations of 17.1, 14.3, and 14.5%, respectively. The predicted solubilities using NRTL and modified Van Laar models provided mean deviations of 44.1 and 47.1%, respectively. The sensitivity analysis showed that the correlations using the NRTL model are slightly influenced by variations up to 20% of the triple-point temperature and molar enthalpy of fusion of the solute.

1. INTRODUCTION

Polycyclic aromatic compounds (PACs) are substances that have more than one benzene aromatic ring structure. PACs include polycyclic aromatic hydrocarbons (PAHs), substituted PAHs, and PAH heterocyclic derivatives. PAHs are a large class of compounds considered as environmental contaminants or pollutants which are composed of two or more fused aromatic rings and do not contain heteroatoms.[1] PACs are produced by human or natural environmental activities by incomplete combustion of organic matter or by oil contamination.[2] Studies have shown that high levels of PACs are found in tobacco smoke, meat cooked at high temperatures such as grilling or barbecuing, smoked fish,[3] etc. Seventeen PAHs (acenaphthene, acenaphthylene, anthracene, benz[*a*]anthracene, benzo[*a*]pyrene, benzo[*e*]pyrene, benzo[*b*]fluoranthene, benzo[*g*,*h*,*i*]perylene, benzo[*j*]fluoranthene, benzo[*k*]fluoranthene, chrysene, dibenz[*a*,*h*]anthracene, fluoranthene, fluorene, indeno[1,2,3-*c*,*d*]pyrene, phenanthrene, and pyrene) are of particular interest as they are considered as a group to have harmful health effects by the Agency for Toxic Substances and Disease Registry.[4]

PACs mix more easily with oil than with water. For example, compounds such as benzo[*a*]anthracene or chrysene are less water-soluble and less volatile. Because of these properties, PACs are found primarily in soil, sediment, and oily substances, as opposed to in water or in the air. However, they are components of concern in particulate matter suspended in the air. Some of these PACs have been identified as carcinogenic, mutagenic, and teratogenic.[5]

Due to their low aqueous solubility, PACs are often resistant to biological degradation[6] and the conventional physicochemical methods of separation are not efficient.[5] As a result, they are accumulated continuously in the environment as in soils and then dispersed by the air. Recently, subcritical water (SCW) has been increasingly used as a green extraction solvent to remove PACs and pesticides from highly contaminated soils.[7] This process relies on the decrease of water polarity with increasing temperature. Increasing the temperature and pressure to maintain the water in the liquid state has a dramatic effect on the solubilities of various compounds. Depending on the temperature, SCW can be effective to selectively extract polar or nonpolar organic compounds from different matrixes. The understanding of the solute + SCW phase behavior is important to selecting the optimum extraction conditions. However, limited experimental solubility data for PACs in water are available in the literature compared to PAC solubilities in other fluids.[8] Hence, a thermodynamic model able to accurately describe the PAC aqueous solubilities is essential to better monitoring the behavior of these compounds at various temperature and pressure conditions. Solubility data are also crucial for an extraction process at the pilot and industrial scales. To date, solubility data of PACs in water at various pressures are scarce.

Empirical and thermodynamic approaches to describe the phase equilibria of PACs in water have been attempted. For their aqueous solubilities, empirical models that can correlate them with specific properties of the pollutants were proposed. For example, Zhao et al.[9] and Chu et al.[10] used simple linear equations, but their models only consider the aqueous solubility at 25 °C to establish the correlation between the solubility and the partition coefficient. Paasivirta et al.[11] developed a temperature-dependent model but within a limited temperature range (0−30 °C). Lu et al.[12] developed two quantum chemical descriptor models to describe the solubilities of 32 PAHs in water. Thermodynamic models such as equations of state (EoS)

Received: May 11, 2011
Accepted: August 16, 2011
Revised: August 10, 2011
Published: August 16, 2011

dx.doi.org/10.1021/ie201019b | *Ind. Eng. Chem. Res.* 2011, 50, 11396–11405

and activity coefficient models can also be used to calculate the aqueous solubilities of PACs. Two EoS, the statistical associating fluid theory (SAFT) and the cubic-plus-association (CPA), were used to describe the solubilities of PAHs in water.[13,14] Oliveira et al.[14] used the CPA model to predict and correlate solubilities of 11 PAHs in SCW with mean deviations of 59.3 and 5.7%, respectively.

One of the major advantages of an EoS compared to activity coefficient models or simple correlations is that it allows the prediction of the solubility in a wide range of pressures and temperatures. However, knowledge of various properties of the pure components is necessary. To simplify the modeling, one alternative is to use fitted activity coefficient models to predict the solubility at other pressures, and should be included the influence of the pressure in the modeling. To date, there are scarce data on modeling of solid−liquid equilibria of PACs + SCW mixtures using activity coefficient models.

Common and industrially important activity coefficient models are the UNIQUAC[15] and NRTL[16] models derived from Guggenheim's method. Among the activity coefficient models nowadays available, UNIQUAC and NRTL have proven to combine simplicity and accuracy required for the prediction and correlation of the solubilities of solids in SCW. During the past 30 years, efforts have been made to extend the applicability of activity coefficient models to obtain accurate representation of phase equilibria in highly polar mixtures, associated mixtures, and other complex systems. The different approaches presented in the literature include the use of multiple interaction parameters in the model,[17,18] the introduction of an empirical temperature-dependent parameter,[19,20] the use of the modified regular solution theory,[21] and the use of empirical equations of biological growth.[22]

The selection of suitable activity coefficient models for solid−liquid phase behavior is important for a reliable representation of solubility behavior. The objective of this study was to investigate the performance of activity coefficient models to predict solubilities of PACs in SCW. A sensitivity analysis of the best models on the accuracy of solubility calculation was also investigated. The activity coefficient models used were UNIQUAC, local surface Guggenheim (LSG),[23] NRTL, Wilson,[24] regular solution (RS) theory,[24] Van Laar (VL),[24] and modified Van Laar (mVL).[25] The results obtained using these model approaches were compared with the ones reported in the literature.

2. MODELS FOR SOLUBILITY CALCULATIONS

The theory of solid solubility in a liquid is found in standard books.[24] The fundamental equation of phase equilibria establishes that, at a given temperature and pressure, the fugacity (f) of a component, for example the solid solute (subscript 2), in the liquid phase must be equal to the fugacity of the same component in the solid phase.

$$f_2^{s} = f_2^{l} \tag{1}$$

In liquid−solid systems, the solid can be considered a pure component, so the fugacity at the temperature T and pressure P for the component 2 is

$$f_2^{s\circ} = \gamma_2 x_2 f_2^{l\circ} \tag{2}$$

where x_2 is the solubility of the solute in the liquid, γ_2 is the activity coefficient of 2, and $f_2^{l\circ}$ is the standard state fugacity to which γ_2 refers. The standard state fugacity $f_2^{l\circ}$ is arbitrary, but conveniently is defined as the fugacity of the pure, subcooled liquid at the temperature of the solution under its own saturation pressure. The equation results in

$$x_2 = \frac{f_2^{s\circ}}{\gamma_2 f_2^{l\circ}} \tag{3}$$

The ratio of the fugacities can be calculated by the thermodynamic cycle of the solute into the liquid:[24,26]

$$\ln\left(\frac{f_2^{s\circ}}{f_2^{l\circ}}\right) = \frac{\Delta H_f}{RT_{tp}}\left(1-\frac{T_{tp}}{T}\right) + \frac{\Delta c_p}{R}\left(\frac{T_{tp}}{T} - 1 - \ln(T_{tp}/T)\right) + \frac{P(v_2^{s\circ} - v_2^{l\circ})}{RT} \tag{4}$$

In eq 4, R is the molar gas constant, P is the pressure, T is the absolute temperature, T_{tp} is the triple-point temperature of the solute, ΔH_f is the molar enthalpy of fusion of the solute at T_{tp}, $v_2^{s\circ}$ and $v_2^{l\circ}$ are the molar volumes of the pure solid solute and the pure subcooled liquid solute, respectively, and Δc_p is the difference in heat capacities ($\Delta c_{p2}^{l\circ} - \Delta c_{p2}^{s\circ}$). The experimental data for $c_{p2}^{l\circ}$ and $c_{p2}^{s\circ}$ are not available for most solutes. Therefore, two suitable approximations were considered, one with $\Delta c_p = 0$ and the other one with Δc_p approximated by the Hurst and Harrison method.[27] The subcooled liquid molar volume, $v_2^{l\circ}$, was estimated from the modified Shah and Yaws equation.[28] The acentric factor and critical properties were estimated using methods proposed by Valderrama et al.[29] and Alvarez and Valderrama,[30] respectively, for organic compounds and ionic liquids. The molar volume of the solid ($v_2^{s\circ}$), needed for the fugacity ratio ($f_2^{s\circ}/f_2^{l\circ}$) calculation, was estimated from the subcooled liquid molar volume ($v_2^{l\circ}$) using the correlation of Goodman et al.[31]

UNIQUAC Model. This model has two main contribution terms—a combinatorial (entropic contribution, related to the molecule size and shape) term and a residual (enthalpic contribution, related to the energy of interactions) term:

$$\gamma_i = \gamma_i^{com} + \gamma_i^{res} \tag{5}$$

$$\gamma_i^{com} = \ln\frac{\Phi_i^*}{x_i} + \frac{z}{2} q_i \ln\frac{\theta_i}{\Phi_i^*} + l_i - \frac{\Phi_i^*}{x_i}\sum_{j=1} x_j l_j \tag{6}$$

$$\gamma_i^{res} = -q_i \ln\left(\sum_{j=1}^{N} \theta_j \tau_{ji}\right) + q_i - q_i \sum_{j=1}^{N} \frac{(\theta_j \tau_{ij})}{\sum_{k=1}^{N} \theta_k \tau_{kj}} \tag{7}$$

$$\Phi_i^* = \frac{r_i x_i}{\sum_j r_j x_j}, \qquad \theta_i = \frac{q_i x_i}{\sum_j q_j x_j}, \tag{8}$$

$$l_j = \frac{z}{2}(r_j - q_j) - (r_j - 1), \qquad \tau_{ij} = \exp\left(-\frac{A_{ij}}{RT}\right) \tag{9}$$

where A_{ij} and A_{ji} are interaction parameters that represent the interaction energy between molecules i and j, Φ_i^* and θ_i are the volume and surface area fractions, respectively, z is the coordination number ($z = 10$), l_j is the bulk factor for component j, and r

and q are the pure-component structural parameters for molecular volume and surface area, respectively.

Local Surface Guggenheim Model (LSG). Vera et al.[23] developed new equations for the excess Gibbs energy of liquid mixtures based on Guggenheim's equation for athermal mixtures and Wilson's local composition concept. The LSG model was used due to its similarity with a previous UNIQUAC model. However, this model calculates the pure-component structural parameters (r, q) from the molar volume at 20 °C. This equation also includes two main terms:

$$\gamma_i = \gamma_i^{\mathrm{com}} + \gamma_i^{\mathrm{res}} \tag{10}$$

$$\gamma_i^{\mathrm{com}} = 1 - \frac{\Phi_i}{x_i} + \ln\frac{\Phi_i}{x_i} + \frac{z}{2} q_i \left(\frac{\Phi_i}{\theta_i} + \ln\frac{\theta_i}{\Phi_i}\right) \tag{11}$$

$$\gamma_i^{\mathrm{res}} = -\frac{zq_i}{2}\left[\sum_{k=1}^{N}\frac{(\theta_k\tau_{ki})}{\sum_{j=1}^{N}\theta_j\tau_{kj}} + \ln\left(\sum_{k=1}^{N}\theta_k\tau_{ik}\right)\right] \tag{12}$$

$$\Phi_i = \frac{r_i x_i}{\sum_j r_j x_j}, \qquad \theta_i = \frac{(zq_i)x_i}{\sum_j (zq_j)x_j}, \qquad \tau_{ij} = \exp\left(-\frac{A_{ij}}{RT}\right) \tag{13}$$

$$zq_i = 0.4228v_i + 2(1 - l_i), \qquad r_i = v_i/v^*, \qquad q_i = a_i/a^* \tag{14}$$

$$v_i = 0.554v_{\mathrm{m}}(20\ ^\circ\mathrm{C}), \qquad a_i = \left(\frac{z-2}{z}\frac{a^*}{v^*}\right)v_i + \frac{2a^*}{z} \tag{15}$$

$$v^* = \frac{z-2}{z}\frac{a^*}{1.323\times 10^8}, \qquad a^* = z(6.259\times 10^8)/2 \tag{16}$$

where A_{ij} and A_{ji} are interaction parameters that represent the interaction energy between molecules i and j, Φ_i^* and θ_i are the volume and surface area fractions, respectively, z is the coordination number ($z = 10$), v_{m} is the molar volume of the compound at 20 °C, v_i is the volume of the molecule, a_i is the surface of the molecule, l_i is the bulk factor for component i ($l_i = 1$ for molecule type ring), and r and q are the pure-component structural parameters for molecular volume and surface area, respectively.

NRTL Model. For a solution of N components, the NRTL model is given by

$$\ln(\gamma_i) = \frac{\sum_j^N G_{ji}\tau_{ji}x_j}{\sum_k^N G_{ki}x_k} + \sum_{j=1}^{N}\frac{x_j G_{ij}}{\sum_k^N G_{kj}x_k}\left[\tau_{ij} - \ln\frac{\sum_{r=1}^{N} G_{rj}\tau_{rj}x_r}{\sum_k^N G_{kj}x_k}\right] \tag{17}$$

$$\tau_{ij} = U_{ij}/(RT), \qquad G_{ij} = \exp(-\alpha_{ij}\tau_{ij}), \qquad \alpha_{ij} = \alpha_{ji} \tag{18}$$

where U_{ij} and U_{ji} are interaction parameters that represent the interaction energy between molecules i and j, and α_{ji} is the nonrandomness parameter.

Regular Solution Model (RS). For a solution of N components, the RS model is given by

$$\ln(\gamma_i) = \frac{v_i\sum_j^N\sum_k^N \Phi_j\Phi_k\left(D_{ji} - \frac{1}{2}D_{jk}\right)}{RT} \tag{19}$$

$$D_{ij} = (\delta_i - \delta_j)^2 + 2l_{ij}\delta_i\delta_j, \qquad \Phi_i = \frac{x_i v_i}{\sum_{j=1}^{N} x_j v_j} \tag{20}$$

where δ_i is the solubility parameter for the pure compound i, v_i is the molar volume of the pure compound i, and l_{ij} is an interaction parameter.

Wilson Model. For a solution of N components, the Wilson model is given by

$$\ln(\gamma_k) = -\ln\left(\sum_{j=1}^{N}\Lambda_{kj}x_j\right) + 1 - \sum_{i=1}^{N}\frac{x_i\Lambda_{ik}}{\sum_{j=1}^{N}\Lambda_{ij}x_j} \tag{21}$$

$$\Lambda_{ij} = \frac{v_j}{v_i}\exp\left(-\frac{A_{ij}}{RT}\right), \qquad \Lambda_{ji} = \frac{v_i}{v_j}\exp\left(-\frac{A_{ji}}{RT}\right),$$
$$A_{ij} = \lambda_{ij} - \lambda_{ii}, \qquad A_{ji} = \lambda_{ji} - \lambda_{jj} \tag{22}$$

where v_i is the molar volume of the pure compound i; λ_{ij} and λ_{ji} represent the interaction energy between molecules i and j.

Van Laar Model (VL). The original Van Laar equation[24] shows some deficiencies. The empirical constants have no physical significance and the Carlson−Colburn form of the Van Laar equation cannot be extended to multicomponent systems without imposing certain unreasonable constraints to the coefficients. The most typical form of this model is

$$\ln(\gamma_1) = \frac{A}{\left(1 + \frac{Ax_1}{Bx_2}\right)^2}, \qquad \ln(\gamma_2) = \frac{B}{\left(1 + \frac{Bx_2}{Ax_1}\right)^2} \tag{23}$$

where A and B are interaction parameters. In this study, the interaction parameters were used as $A = a/RT$ and $B = b/RT$.

Modified Van Laar Model (mVL). Peng[25] modified the original Van Laar equation to multicomponent systems.

$$\ln(\gamma_k) = \frac{b_k}{\sum_{i=1}^{N} x_i b_i}\left[\sum_{\substack{i=1\\ i\neq k}}^{N} x_i b_i \varepsilon_{ik} - \frac{G^{\mathrm{E}}}{RT}\right] \tag{24}$$

$$\frac{G^{\mathrm{E}}}{RT} = \frac{\sum_{i}^{N-1}\sum_{j=i+1}^{N} x_i x_j b_i b_j \varepsilon_{ij}}{\sum_{i=1}^{N} x_i b_i} \tag{25}$$

where b_i, b_j and ε_{ij} are the interaction parameters of the model and G^{E} is the excess Gibbs free energy. In this study, the three empirical parameters were fitted to the experimental data. Two parameters were used as $b_i = A_i/RT$ and $b_j = A_j/RT$.

Table 1. Properties of Water and PACs[a]

compound	M (g/mol)	T_b (K)	T_c (K)	P_c (bar)	V_c (cm^3/mol)	ref	δ(25 °C) (J/cm^3)$^{0.5}$	T_{tp} (K)	ΔH (J/mol)	r	q	ref	Δc_p[27] (J/(molK))	α_s[35] (nm^3)
water	18.015	373.150	647.130	220.550	55.950	33	47.810					33		
1,2-benzanthracene	228.293	710.750	979.000	23.900	690.000	33	21.900	433.550	2.140×10^4	8.251	5.304	33	59.10	2.95×10^{-2}
4,6-DMDBT	212.310	651.180	1112.640	30.169	686.060	29	21.296	463.130	2.346×10^4	7.720	5.281	34	70.03	2.65×10^{-2}
acridine	179.221	619.150	905.000	36.400	543.000	33	20.200	383.240	2.068×10^4	6.374	4.028	33	54.68	2.25×10^{-2}
anthracene	178.233	615.180	873.000	29.000	554.000	33	17.730	488.930	2.937×10^4	6.563	4.336	33	47.06	2.32×10^{-2}
carbazole	167.210	627.865	899.000	32.600	482.000	33	20.820	517.950	2.943×10^4	6.320	4.828	33	52.49	2.10×10^{-2}
chrysene	228.293	714.150	979.000	23.900	749.000	33	18.920	531.150	2.620×10^4	8.251	5.304	33	59.10	2.95×10^{-2}
dibenzofuran	168.195	558.310	824.000	36.400	495.000	33	19.760	355.310	1.929×10^4	5.711	3.752	33	41.98	2.04×10^{-2}
dibenzothiophene	184.262	604.609	897.000	38.600	512.000	33	20.010	371.820	2.158×10^4	6.137	3.828	33	59.09	2.28×10^{-2}
fluoranthene	202.255	655.950	905.000	26.100	655.000	33	19.290	383.330	1.873×10^4	7.188	4.504	33	51.44	2.62×10^{-2}
fluorene	166.222	570.440	826.000	30.000	524.000	33	19.820	387.940	1.958×10^4	6.175	4.076	33	44.87	2.17×10^{-2}
naphthalene	128.174	491.143	748.400	40.500	407.000	33	19.490	353.430	1.898×10^4	4.920	3.368	33	35.02	1.68×10^{-2}
perylene	252.310	689.520	1224.809	43.800	658.310	29	21.674	550.150	3.258×10^4	9.048	5.621	34	63.48	3.26×10^{-2}
phenanthrene	178.233	610.030	869.000	29.000	554.000	33	19.910	372.380	1.646×10^4	6.563	4.336	33	47.06	2.32×10^{-2}
phenanthridine	179.220	581.600	970.487	50.040	502.330	29	24.169	379.940	2.283×10^4	6.530	4.353	34	54.68	2.25×10^{-2}
phenazine	180.210	612.420	1042.920	56.935	501.930	29	26.184	444.000	2.092×10^4	6.397	4.292	34	62.30	2.19×10^{-2}
phenothiazine	199.270	667.660	1090.669	33.752	629.910	29	22.916	458.390	2.566×10^4	6.793	4.579	34	72.18	2.40×10^{-2}
phenoxathiin	200.260	646.060	1072.776	32.183	619.710	29	22.738	328.770	2.027×10^4	6.688	4.513	34	61.67	2.34×10^{-2}
phenoxazine	183.210	581.360	930.028	52.013	462.650	29	23.380	429.850	3.087×10^4	6.398	4.337	34	55.07	2.16×10^{-2}
p-terphenyl	230.309	655.150	908.000	29.900	729.000	33	17.860	485.000	3.370×10^4	8.899	6.104	33	62.38	2.99×10^{-2}
pyrene	202.255	667.950	936.000	26.100	660.000	33	19.670	423.810	1.736×10^4	7.188	4.504	33	51.44	2.62×10^{-2}
thianthrene	216.320	732.360	1244.274	23.292	786.970	29	22.336	429.570	2.756×10^4	7.087	4.758	34	78.78	2.58×10^{-2}
triphenylene	228.290	646.880	1080.620	40.565	623.070	29	21.283	471.010	2.474×10^4	8.398	5.427	34	59.10	2.95×10^{-2}

[a] 4,6-DMDBT, 4,6-dimethyldibenzothiophene; M, molar mass; T_b, normal boiling temperature; T_c, critical temperature; P_c, critical pressure; V_c, critical volume; δ, Hansen solubility parameter; T_{tp}, triple-point temperature of the solute; ΔH, sublimation enthalpy; r, UNIQUAC volume parameter; q, UNIQUAC area parameter; Δc_p, difference between solid and liquid heat capacity; α_s, polarizability.

3. MINIMIZATION USING GENETIC ALGORITHMS

The genetic algorithm, a numerical method intended to mimic some processes of natural evolution and species selection, was adopted from Alvarez et al.[32] with slight modifications. In this study, the calculation of the interaction parameters started with a set of 80 solutions (population). Each solution (individual) has a random value inside the interval of solutions for each binary interaction parameter of the model. The solution of the model for the binary interaction parameter and the nonrandomness parameter ranges from -10^6 to 10^6 and from 0.2 to 0.55, respectively. Each individual solution consists of a set of variables (chromosomes) that represent the value of each parameter to be calculated. The population in each iteration (generation) is improved to minimize the objective function for each of the individuals. The creation of new solutions (offspring) by crossover and mutation was carried out for each generation. The parents were replaced by the offspring to produce a new generation. The criterion to stop the calculation was 10 000 generations.

For the thermodynamic model, eq 4 was used in this study. The objective function was defined as the difference between experimental and calculated values. The average percent deviation of this difference was expressed in absolute form for a set of N experimental points, as in eq 26.

$$|\Delta x_2|\% = \frac{100}{N}\sum_{i=1}^{N}\left[\frac{|x_2^{cal} - x_2^{exp}|}{x_2^{exp}}\right]_i \quad (26)$$

where x_2^{cal} and x_2^{exp} are the calculated and experimental concentrations of the solute, respectively.

4. SENSITIVITY ANALYSIS

Sensitivity analysis was used to determine if the thermodynamic model was affected by changes in the values of pure solid properties and changes in the structure of the model. Sensitivity analysis was performed using different parameter values to observe how a change in a parameter caused a change in the dynamic behavior of the dependent variable. For the sensitivity analysis, the dependent variable average percentage deviation of the fit was used. The independent parameters (known as factors) studied were the following: T_{tp} (the triple-point temperature of the solute), ΔH_f (the molar enthalpy of fusion of the solute at T_{tp}), $v_2^{s\circ}$ and $v_2^{l\circ}$ (the molar volumes of the pure solid solute and the pure subcooled liquid solute, respectively), and Δc_p (the difference between $\Delta c_{p2}^{l\circ}$ and $\Delta c_{p2}^{s\circ}$).

The main effect of the independent variables (contribution of each factor) and their interactions (contribution of interaction between factors) on the dependent variable ($|\Delta x_2|\%$) were also investigated by preparing a Pareto chart. A positive value indicates that the increase of the main or interaction effects causes an increase of the dependent variable. A negative value indicates the opposite behavior. The sensitivity analysis of the thermodynamic model was studied at lower and upper limit values for these five independent parameters using a full factorial design. Thirty-two experimental settings of 2^5 factorial points were generated with five factors and two levels using the software Statistica 7. The sensitivity analysis was carried out with the NRTL and mVL models for the binary system water + naphthalene. The code levels −1 and +1 (lower and upper levels) were the properties of the naphthalene with a decrease and an increase of 10% (lower and upper values), respectively.

Table 2. Range (Ω) of the Experimental Data for the Systems Considered in This Study[a,b]

system: water +	N	$\Omega(T)$ (K)	$\Omega(P)$ (bar)	$\Omega(x_2) \times 10^8$	ref
1,2-benzanthracene	7	313−423	48−52	3.4−159.8	21
4,6-DMDBT	7	313−423	50	0.32−515.0	37
acridine	4	313−363	50	909.9−6087.0	26
anthracene	15	313−473	47−54	1.2−22 020.0	21
	4*[c]	298−413	1−77	0.7−13 050.0	19, 38
carbazole	7	313−433	50−52	27.2−16 830.0	26
chrysene	5	298−473	32−45	0.06−1580.0	21
dibenzofuran	5	313−353	50−52	91.7−704.2	26
dibenzothiophene	6	313−363	50−52	20.6−348.7	26
fluoranthene	5	313−378	49−50	4.0−188.7	26
fluorene	6	313−383	49−50	38.2−1579.0	26
naphthalene	8	313−348	50−51	692.2−4353.0	21
	5*[c]	298−338	30−70	463.4−3036.0	19
perylene	4	323−473	47−50	0.003−500	21
	1*[c]	298	1	0.003	
phenanthrene	5	313−363	50	21.7−327. 1	26
phenanthridine	4	313−363	50	628.7−5921.0	26
phenazine	7	313−433	49−50	717.3−82 750.0	26
phenothiazine	8	313−353	50−51	29.2−43 150.0	26
phenoxathiin	4	313−328	50	27.8−75.1	26
phenoxazine	6	313−413	50	194.0−22 300.0	37
p-terphenyl	8	333−483	49−54	0.08−3932.0	21
	1*[c]	433	67	154.2	
pyrene	6	298−413	41−50	1.1−540.0	21
	2*[c]	298−373	1−200	1.2−78.0	
thianthrene	7	313−423	48−56	1.5−1607.0	26
triphenylene	10	313−468	50−64	18.2−2828.0	21

[a] The temperature (T) and pressure (P) values were rounded to the closest integer. [b] N, data number; x_2, mole fraction of the PAC in water. [c] Experimental data used for the prediction test.

5. RESULTS AND DISCUSSION

Modeling. The interaction parameters of the activity coefficient models were calculated by regression analysis of experimental phase equilibrium data. The objective function for the phase equilibrium of a liquid−solid system that includes the solute concentration in the liquid phase was minimized using a genetic algorithm code described in section 3.

Table 1 provides the main properties of water and 22 PACs selected, such as the molar mass M, the normal boiling temperature T_b, the critical temperature T_c, and the critical pressure P_c. Most of the data were obtained from Diadem,[33] calculated using the Valderrama et al.[29] method, the Alvarez and Valderrama method,[30] or the Molecular Modeling Pro software.[34] The polarizability value (α_s) was calculated using the method proposed by Bosque and Sales.[35] Table 1 shows that there is an increase of the normal boiling temperature, the triple-point temperature, the molar enthalpy of fusion, and polarizability values with the increase of the molar mass.

Table 2 provides information on the experimental data used to model. In Table 2, N is the number of experimental data for each binary system, $\Omega(T)$ is the interval temperature (expressed in kelvin), $\Omega(P)$ is the range in pressure (expressed in bar), and $\Omega(x_2)$ is the liquid mole fraction range for component "2".

Table 3. Deviations in the Liquid Phase Concentration of the Solute (x_2) for the Systems Studied Using Models Based on Activity Coefficient without Δc_p

	Δx_2[a] (%)					
system: water (1) +	UNIQUAC	LSG	NRTL	RS	Wilson	VL
1,2-benzanthracene	45.9	32.0	22.9	33.6	12.3	13.8
4,6-DMDBT	49.0	34.2	22.2	32.0	10.5	11.5
acridine	11.1	7.6	7.6	11.0	25.7	13.8
anthracene	51.2	44.3	30.7	48.1	32.3	30.9
carbazole	33.8	28.6	13.0	25.2	5.9	7.3
chrysene	51.2	50.7	59.2	61.0	43.0	45.2
dibenzofuran	10.1	6.2	5.4	6.4	43.4	6.9
dibenzothiophene	18.8	5.8	4.8	6.0	24.3	6.6
fluoranthene	35.7	14.0	6.4	14.6	30.2	6.6
fluorene	32.5	14.3	1.6	15.6	30.3	4.8
naphthalene	14.9	8.5	1.9	12.3	21.9	2.0
perylene	48.2	60.2	58.2	66.2	38.1	36.4
phenanthrene	21.2	7.3	3.1	8.2	21.7	3.8
phenanthridine	3.8	3.5	3.8	4.9	21.7	7.8
phenazine	33.2	16.1	10.0	12.9	11.3	12.2
phenothiazine	46.6	30.8	13.2	27.1	13.2	11.4
phenoxathiin	8.2	3.8	1.2	2.8	38.3	1.0
phenoxazine	19.6	10.6	10.7	11.2	16.8	15.7
p-terphenyl	62.5	50.5	37.1	57.2	35.6	26.5
pyrene	43.5	21.7	18.4	63.2	24.2	20.5
thianthrene	43.4	25.7	13.6	21.1	8.6	7.8
triphenylene	63.1	44.9	32.0	43.9	24.1	22.6
mean	34.0	23.7	17.1	26.6	24.2	14.3

[a] UNIQUAC, universal quasi-chemical; LSG, local surface Guggenheim; NRTL, nonrandom two-liquid; RS, regular solution; VL, Van Laar.

Table 2 shows that the experimental data to fit each binary system was approximately isobaric ($\Delta P \approx 5$ bar), and the literature data with the (*) symbol were used for prediction using the fitted models. The compounds used for the prediction test were selected according to availability of data at various pressures. In addition, Table 2 shows that the majority of literature studies used a range of temperature from 313 to 480 K and a range of pressure from 40 to 60 bar with a lack of data at low (<20 bar) and high (>100 bar) pressures. Table 2 also shows that a compound with a high polarizability value (Table 1) has a low solubility in SCW. For example, at 50 bar and 313 K, the solubilities of naphthalene ($\alpha_s = 0.0168$) and 4,6-DMDBT ($\alpha_s = 0.0265$) are 6.92×10^{-6} and 0.32×10^{-8}, respectively. Therefore, SCW as a remediation technology is limited for PACs of low polarizability values.

The modeling of the binary systems was carried out with two considerations, neglecting or using the term Δc_p in the model (eq 4). Table 3 shows the results of six models, neglecting Δc_p, while Table 4 shows the results with and without Δc_p for the mVL model. Tables 3 and 4 show the average absolute deviations for the solute concentration in the liquid phase, $|\Delta x_2|$%. The interaction parameters obtained for the systems studied herein are provided in the Supporting Information. Tables 3 and 4 show that the better fitted deviations for the 22 binary systems were obtained using the NRTL, VL, and mVL models, with mean deviations of 17.1, 14.3, and 14.5%, respectively. NRTL, VL, and

Table 4. Solubility Comparison of the Solute (x_2) in SCW for the Systems Studied Using the Modified Van Laar Model with and without Δc_p[a]

	without Δc_p (mVL)				with Δc_p (mVL-c_p)			
system: water (1) +	ε_{ij}	A_j (J/mol)	A_i (J/mol)	Δx_2 (%)	ε_{ij}	A_i (J/mol)	A_j (J/mol)	Δx_2 (%)
1,2-benzanthracene	0.2189	24.5699	212 200.9219	13.4	0.2152	27.4667	215 277.0938	19.5
4,6-DMDBT	0.2199	31.8655	197 067.2656	11.5	0.2229	21.4585	201 283.2656	19.5
acridine	0.1411	−219.7257	184 567.8438	6.4	−0.1134	−329.5907	232 827.8594	5.3
anthracene	0.2241	558.8659	169 464.1094	30.9	0.2306	463.4865	168 897.2031	33.6
carbazole	0.1316	1052.2850	214 782.7188	6.7	−0.8156	−111.7936	−36 585.1172	14.3
chrysene	0.2228	54.9325	203 803.2500	52.2	0.1646	54.9325	290 392.6875	47.1
dibenzofuran	0.1618	−273.3699	211 761.4688	7.0	0.1624	−356.0356	211 478.6562	6.4
dibenzothiophene	−0.2134	54.9325	−173 344.5156	6.6	0.1742	−123.5954	213 684.0781	5.2
fluoranthene	0.2235	710.6790	184 933.8125	6.6	0.2324	61.1552	178 739.4062	4.7
fluorene	0.1611	−3953.7361	217 474.3594	4.8	0.1664	892.5327	211 788.9375	3.3
naphthalene	−0.4567	−887.4885	−63 198.6914	2.0	−0.3925	−662.5048	−73 712.5781	2.0
perylene	0.2983	10.3005	170 251.8281	38.9	0.2406	13.9483	209 944.8750	56.2
phenanthrene	−0.6558	1179.0448	31.9209	3.8	0.1737	659.1805	217 286.5000	2.6
phenanthridine	−0.1109	1414.0614	−249 829.0938	6.0	−0.1238	1757.2769	−225 439.4062	4.7
phenazine	−0.1209	−8789.0078	−214 874.9844	11.4	−0.0801	−9002.8340	−330 909.7188	5.4
phenothiazine	0.1708	1650.7395	185 431.2031	11.8	−0.3940	−530.0903	−83 313.5625	14.5
phenoxathiin	0.1878	−110.1843	203 521.7344	1.1	0.4422	−54.9308	86 446.4141	1.0
phenoxazine	−0.1183	91916.5156	−233 133.7969	15.7	0.1597	5825.5444	175 341.7969	10.7
p-terphenyl	0.1583	164.7958	292 675.7812	32.2	0.1663	116.7306	294 028.7812	36.1
pyrene	0.1942	192.2616	214 288.2188	20.4	0.2236	399.1135	184 844.9688	17.5
thianthrene	0.2188	132.1801	182 839.9688	6.9	0.1899	115.0140	213 862.6094	8.1
triphenylene	0.2249	117.0524	197 556.9219	22.5	−0.7518	−27.4657	60 792.8398	28.2
mean				14.5				15.7

[a] A_i, B_j, and ε_{ij} are the interaction parameters of the model.

mVL models contain three, two, and three fitted interaction parameters, respectively. Also, in Table 3, for the Guggenheim based methods, the LSG model had better correlation than the UNIQUAC model with a mean deviation of 34.0%. This might be attributed to errors in the theoretical development of the calculation of the structural parameters and the residual contributions of the model.[36] For the 22 systems studied, the maximum deviations were obtained for chrysene, perylene, and *p*-terphenyl with mean deviations of 52.2, 38.9, and 32.2%, respectively, using the mVL model. These compounds have low solubility in SCW compared to the other PACs. Then, the high deviations are the result of the lack of accuracy of the activity coefficient determination. The predominance of the ideal solubility behavior is evident using the UNIQUAC (34%) compared to the VL (18%) model. Table 4 shows deviations of the fitted solubility using mVL with the Δc_p in the model (mVL-c_p). Similar deviations of 14.5 and 15.7% for mVL and mVL-c_p were obtained, respectively. Then, the use of the Δc_p in the model did not improve the fit of PAC solubility in SCW.

Figures 1 and 2 show the temperature versus the PAC concentration for the mixture water (1) + phenazine (2) at 50 bar, and for water (1) + naphthalene (2) at various pressures, respectively. The symbols represent the experimental data, and the lines represent the calculated solubility values. Figure 1 shows good agreement of all models at low temperatures for low solute solubility. At high temperatures, UNIQUAC, LSG, RS, and Wilson models have high deviations of the aqueous solubility; this behavior shows that the algebraic expression containing the temperature parameter in each of these models might not be accurate. This hypothesis can be supported for a simplified UNIQUAC model that generates low deviations. In fact, if the combinatorial term is equal to zero in the UNIQUAC model, it reduces to NRTL, VL, or RS models.[15] In addition, Figure 1 shows that the best fittings in the whole temperature interval were obtained using NRTL and Van Laar based models.

The results using the NRTL model showed that the systems with low solubility values have high deviations. However, the same systems have low deviations using the VL model. The limitation of the NRTL model is the α_{12} value interval from 0.20 to 0.55 as well explained by Renon and Prausnitz.[16] Good correlations with the Van Laar model were obtained because the interaction parameters are directly proportional to the infinity activity coefficient values. Also, the Van Laar model provides a good fit for diluted systems such as the ones used in this study.

The UNIQUAC model presents two main theoretical sources of errors that can influence the high deviations of the fit. The first is an assumption of the coordination number (z) into the interaction parameter (A_{ij}) for the residual contribution. The other is that the values of the structural parameters (r, q) generate values for the bulk factor (l_j) different from the unity for ring molecules. These theoretical errors are more evident in dilute or aqueous systems. However, these errors were avoided for the LSG model development, showing lower deviations of the fit than the UNIQUAC model.

Figure 2 shows the predicted solute concentration (x_2) of naphthalene in SCW using the UNIQUAC and mVL-c_p models.

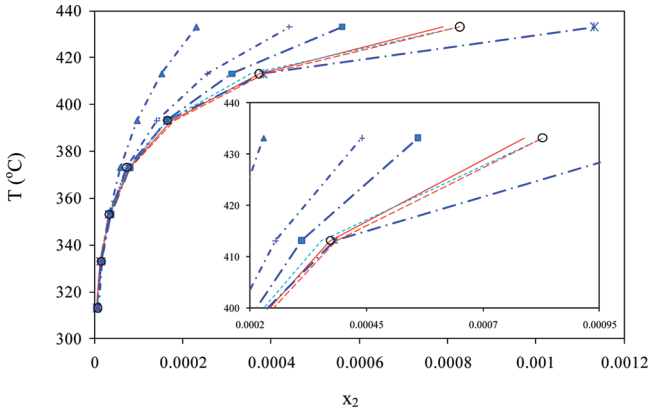

Figure 1. Experimental data (○) and calculated values of temperature vs liquid molar fraction of the solute for the system water (1) + phenazine (2). UNIQUAC (blue — · —▲), LSG (blue — · —+), NRTL (red —), RS (blue — · —■), Wilson (blue — · —∗), VL (red — — —), and mVL-c_p (blue ---) models.

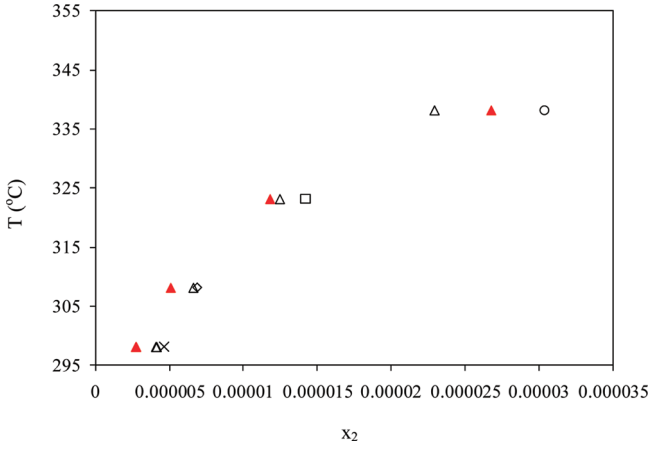

Figure 2. Experimental data and predicted values vs molar fractions of naphthalene. Values for the fitted model at 50 bar and predicted values using UNIQUAC (△) and mVL-c_p (red ▲) models. Experimental data (○) at 30 bar and 338.15 K, (◇) at 40 bar and 308.15 K, (×) at 65 bar and 298.15 K, and (□) at 70 bar and 323.15 K.

Good agreement between UNIQUAC and mVL-c_p predicted values and the experimental data were observed, with mean deviations of 12.7 and 26.8%, respectively. The UNIQUAC model provided better results at low temperatures, while the mVL-c_p model maintained the same deviations for the whole temperature range tested in this study. Table 5 shows the mean relative deviations of the predicted solute concentration in the mixture studied using seven activity coefficient models. The systems predicted were selected based on data availability for different pressures. The model predicted a decrease of the solubility with an increase of the pressure. Then, these models can complement the understanding of the solubility behavior for the PACs in SCW. In Table 5, the mVL model using the Δc_p shows a better prediction with a mean deviation of 35.4%. Furthermore, the low deviations of predicted values were obtained for binary systems with low polarizability values. The deviation values obtained in this study for prediction were similar to those values reported using models such as the correlation model based on the modified regular solution theory (43.7%),[21]

Table 5. Deviations of the Predicted Liquid Phase Concentration of Solute x_2 for Some Systems Studied

water (1) +	UNIQUAC	LSG	NRTL	RS	Wilson	VL	mVL	mVL-c_p
anthracene	58.9	53.2	41.1	56.3	40.0	42.4	42.4	42.4
naphthalene	12.7	21.9	30.1	7.7	36.0	29.8	26.8	28.6
perylene	198.6	36.8	92.1	86.2	85.4	92.0	89.9	33.3
p-terphenyl	87.7	74.4	47.6	79.5	68.6	46.7	46.9	68.3
pyrene	36.56	13.95	9.5	39.0	32.7	25.6	29.6	4.5
mean	78.9	40.1	44.1	53.7	52.5	47.3	47.1	35.4

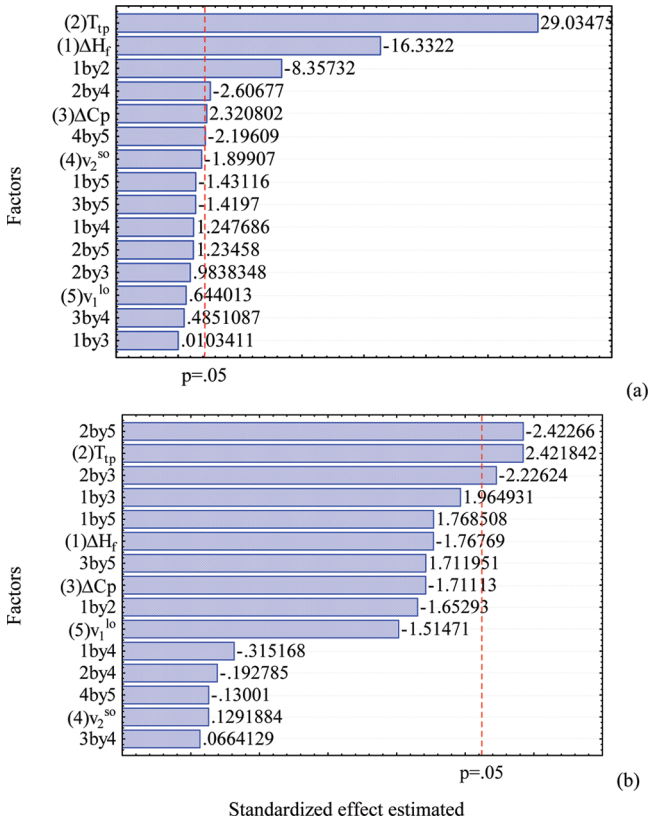

Figure 3. Pareto chart of standardized effects for naphthalene in SCW using the (a) mVL and (b) NRTL models.

the simple first-order group contribution method (35.4%),[26] and the CPA EoS model (59.0%).[14]

Sensitivity Analysis. The standardized Pareto chart of the effects was performed to assess the significance of the independent variables and their two-way interactions (effects) on the deviation of the fit as explained in section 4. This chart provides the effect for each parameter, sorted from the most significant to the least significant. The length of each effect is proportional to the standardized effect, which is equal to the magnitude of the *t*-statistics. A vertical line is drawn at the location of the 0.05 critical value for Student's *t* test. Any bar that extends to the right of that line indicates effects that are statistically significant at the 5% significance level.

In Figure 3, for the mVL and NRTL models, there are six and three effects with *p*-values above 0.05, respectively. The T_{tp} (factor 2), ΔH_f (factor 1), and their interactions (factor 1by2) show important contributions for the deviation using the mVL

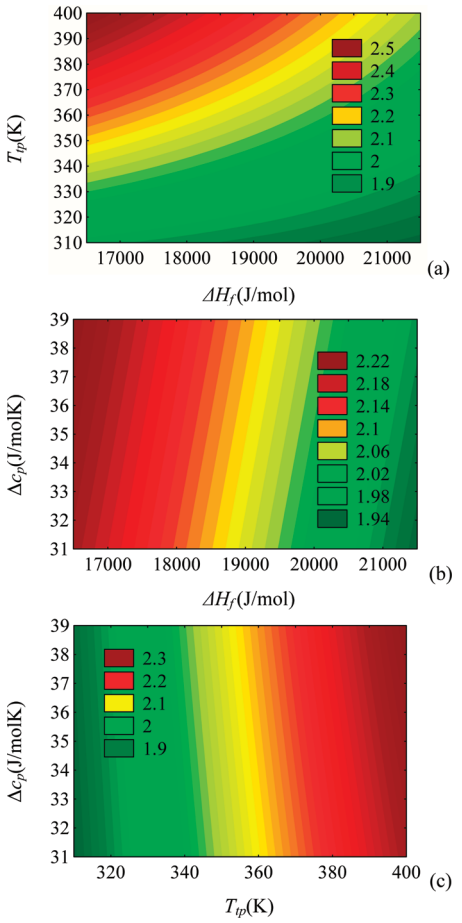

Figure 4. Estimated contour plot in the full 2^5 experimental design obtained for the fit deviation of the mVL model: (a) triple-point temperature of the solute versus molar enthalpy of fusion of the solute at T_{tp}, (b) variation of the heat capacity versus molar enthalpy of fusion of the solute at T_{tp}, and (c) variation of the heat capacity versus the triple-point temperature of the solute.

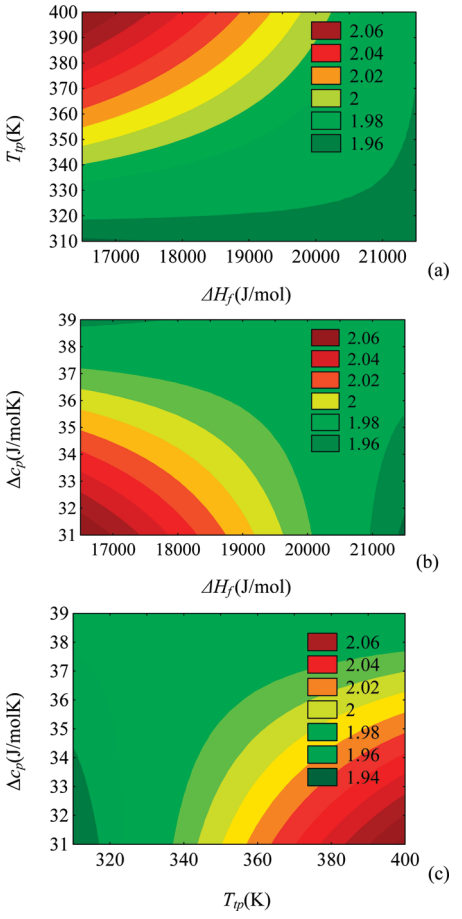

Figure 5. Estimated contour plot in the full 2^5 experimental design obtained for the fit deviation of the NRTL model: (a) triple-point temperature of the solute versus molar enthalpy of fusion of the solute at T_{tp}, (b) variation of the heat capacity versus molar enthalpy of fusion of the solute at T_{tp}, and (c) variation of the heat capacity versus the triple-point temperature of the solute.

model, while the T_{tp} (factor 2) and its interactions with $v_1^{l\circ}$ (factor 2by5) show little contribution for the deviation using NRTL. These results confirmed that the deviation of the fit is slightly influenced by values of the liquid or solid volume of the PAC.

The effect of some factors was also well displayed by a contour plot as presented in Figures 4 and 5 for the mVL and NRTL models, respectively. Figures 4 and 5 show that high values of ΔH_f and low values of T_{tp} result in low values for the deviation of the fit (Figures 4a and 5a). Furthermore, variations of Δc_p at a constant ΔH_f or at a constant T_{tp} do not show any influence using the mVL model (Figure 4b,c). However, the same variations show a slight influence using the NRTL model (Figure 5a,b). In addition, the NRTL model (Figure 5) shows smaller deviations of the fit (1.9−2.1%) than the mVL model (1.9−2.5%) when modifications up to 20% of the PAC properties were used.

The use of Δc_p had no effect on the fit because the Δc_p value was low compared to the high value of ΔH_f. In addition, in the second term of eq 4, the value inside the parentheses is <1. However, for a good solubility prediction, interaction parameters of the specific model using Δc_p are required to describe better the physical phenomena than less empirical models.

The results show that models based on NRTL or VL achieved the best correlations on PAC solubility in SCW compared to the other five models examined in this study. The exactitude for values of the molar enthalpy and temperature at the triple point are critical to achieve good performance of these activity coefficient models. Therefore, new activity coefficient models based on these two theoretical approaches can be further studied to improve predictions of PAC solubility in SCW.

6. CONCLUSIONS

Solid−liquid equilibria for binary mixtures of PACs + subcritical water were modeled by using seven activity coefficient models. Low deviations were found using the activity coefficient method based on NRTL or Van Laar type equations for PAC solubility in SCW. The aqueous solubility of a PAC is directly proportional to the polarizability of the solute. This solubility can be obtained with good accuracy using the modified Van Laar model, with mean absolute average deviations below 14.5% for the 22 systems studied. The solute concentration in the liquid phase, x_2, can be predicted with accuracy at other pressures using mVL-c_p, with absolute mean deviations below 35.4% for the systems studied. Furthermore, the use of the Δc_p had no significant effect on the fit, but improved the prediction, at other pressures, for the systems studied. The interaction parameters

dx.doi.org/10.1021/ie201019b |*Ind. Eng. Chem. Res.* 2011, 50, 11396–11405

obtained by the mVL model, including Δc_p, provided more phenomenological information that was reliable and able to predict PAC solubility in SCW accurately at any other temperature and pressure condition. The sensitivity analysis of the thermodynamic model showed that high values of ΔH_f and low values of T_{tp} produced low deviations of the fit.

■ ASSOCIATED CONTENT

Supporting Information. Tables showing the deviations in the liquid phase concentration of solute (x_2) for the systems studied using UNIQUAC, LSG, NRTL, regular solution, Wilson, and Van Laar models are available. This material is available free of charge via the Internet at http://pubs.acs.org.

■ AUTHOR INFORMATION

Corresponding Author

*Tel.: (780) 492-8018. Fax: (780) 492-8914. E-mail: marleny@ualberta.ca.

■ ACKNOWLEDGMENT

The authors are grateful to the Natural Science and Engineering Research Council of Canada (NSERC) and to Alberta Innovates-Bio Solutions for funding this project.

■ NOMENCLATURE

Symbols

G^E = excess Gibbs free energy
H_f = molar enthalpy of fusion
l_j = bulk factor of component j
M = molar mass (g/mol)
P = pressure (bar)
P_{ci} = critical pressure of component i (bar)
R = ideal gas constant
r = volume pure component structural parameter
q = area pure component structural parameter
T = temperature (K)
T_{tp} = triple-point temperature of the solute (K)
T_{ci} = critical temperature of component i (K)
V = molar volume (cm^3/mol)
Z_c = critical compressibility factor
x_i, x_j = mole fractions of components i and j
N = number of points in a data set
f_2^s = fugacity of the solute in the solid phase
f_2^l = fugacity of the solute in the liquid phase
$v_2^{s\circ}$ = solid molar volume (cm^3/mol)

Abbreviations

LSG = local surface Guggenheim
mVL = modified Van Laar
NRTL = nonrandom two-liquid
RS = regular solution
SCW = subcritical water
UNIQUAC = universal quasi-chemical
VL = Van Laar

Greek Symbols

Δ = deviation
γ_2 = activity coefficient of the solute

Superscripts and Subscripts

exp = experimental
cal = calculated
s = solid phase
l = liquid phase

■ REFERENCES

(1) Fetzer, J. C. The Chemistry and Analysis of the Large Polycyclic Aromatic Hydrocarbons. *Polycyclic Aromatic Compounds*; Wiley: New York, 2000.

(2) Perez, C.; Velando, A.; Munilla, I.; Lopez-Alonso, M.; Oro, D. Monitoring Polycyclic Aromatic Hydrocarbon Pollution in the Marine Environment after the Prestige Oil Spill by Means of Seabird Blood Analysis. *Environ. Sci. Technol.* **2008**, *42*, 707.

(3) Larsson, B. K.; Sahlberg, G. P.; Eriksson, A. T.; Busk, L. A. Polycyclic Aromatic Hydrocarbons in Grilled Food. *J. Agric. Food Chem.* **1983**, *31*, 867.

(4) http://www.atsdr.cdc.gov/ToxProfiles/TP.asp?id=122&tid=25#top (accessed Feb 1, 2011).

(5) Luch, A. *The Carcinogenic Effects of Polycyclic Aromatic Hydrocarbons*; Imperial College Press: London, 2005.

(6) Johnsen, A. R.; Wick, L. Y.; Harms, H. Principles of Microbial PAH-degradation in Soil. *Environ. Pollut.* **2005**, *133*, 71.

(7) Moreno, E.; Reza, J.; Trejo, A. Extraction of Polycyclic Aromatic Hydrocarbons from Soil using Water under Subcritical Conditions. *Polycyclic Aromat. Compd.* **2007**, *27*, 239.

(8) Saldaña, M. D. A.; Nagpal, V.; Guigard, S. E. Remediation of contaminated soils using supercritical fluid extraction: A Review (1994−2004). *Environ. Technol.* **2005**, *26*, 1013.

(9) Zhao, H. X.; Zhang, Q.; Chen, J. P.; Xue, X. Y.; Liang, X. M. Prediction of Octanol-Air Partition Coefficients of Semivolatile Organic Compounds Based on Molecular Connectivity Index. *Chemosphere* **2005**, *59*, 1421.

(10) Chu, W.; Chan, K. H. The Prediction of Partitioning Coefficients for Chemicals Causing Environmental Concern. *Sci. Total Environ.* **2000**, *248*, 1.

(11) Paasivirta, J.; Sinkkonen, S.; Mikkelson, P.; Rantio, T.; Wania, F. Estimation of Vapor Pressures, Solubilities and Henry's Law Constants of Selected Persistent Organic Pollutants as Function of Temperature. *Chemosphere* **1999**, *39*, 811.

(12) Lu, G.-N.; Dang, Z.; Tao, X.-Q.; Yang, C.; Yi, X.-Y. Estimation of Water Solubility of Polycyclic Aromatic Hydrocarbons using Quantum Chemical Descriptors and Partial Least Squares. *QSAR Comb. Sci.* **2008**, *27*, 618.

(13) Economou, I. G. Statistical Associating Fluid Theory: A Successful Model for the Calculation of Thermodynamic and Phase Equilibrium Properties of Complex Fluid Mixtures. *Ind. Eng. Chem. Res.* **2002**, *41*, 953.

(14) Oliveira, M. B.; Oliveira, V. L.; Coutinho, J. A. P.; Queimada, A. J. Thermodynamic Modeling of the Aqueous Solubility of PAHs. *Ind. Eng. Chem. Res.* **2009**, *48*, 5530.

(15) Abrams, D. S.; Prausnitz, J. M. Statistical Thermodynamics of Liquid-Mixtures. New Expression for Excess Gibbs Energy of Partly or Completely Miscible Systems. *AIChE J.* **1975**, *21*, 116.

(16) Renon, H.; Prausnitz, J. M. Local Compositions in Thermodynamics Excess Functions for Liquid Mixtures. *AIChE J.* **1968**, *14*, 135.

(17) Chen, C.-C. A Local Composition Model for the Excess Gibbs Energy of Aqueous Electrolyte Systems. I: Single Completely Dissociated Electrolyte Single Solvent Systems. *AIChE J.* **1982**, *28*, 588.

(18) Chen, C.-C.; Evans, L. N. A Local Composition Model for the Excess Gibbs Energy of Aqueous Electrolyte Systems. *AIChE J.* **1986**, *32*, 444.

(19) Miller, D. J.; Hawthorne, S. B.; Gizir, A. M.; Clifford, A. A. Solubility of Polycyclic Aromatic Hydrocarbons in Subcritical Water from 298 to 498 K. *J. Chem. Eng. Data* **1998**, *43*, 1043.

(20) Hovorka, Š.; Dohnal, V.; Roux, A. H.; Roux-Desgranges, G. Determination of Temperature Dependence of Limiting Activity Coefficients for a Group of Moderately Hydrophobic Organic Solutes in Water. *Fluid Phase Equilib.* **2002**, *201*, 135.

(21) Karásek, P.; Planeta, J.; Roth, M. Solubility of Solid Polycyclic Aromatic Hydrocarbons in Pressurized Hot Water: Correlation with Pure Component Properties. *Ind. Eng. Chem. Res.* **2006**, *45*, 4454.
(22) Lu, L.-L.; Lu, X.-Y. Solubilities of Gallic Acid and Its Esters in Water. *J. Chem. Eng. Data* **2007**, *52*, 37.
(23) Vera, J. H.; Sayegh, S. G.; Ratcliff, G. A. A Quasi Lattice-Local Composition Model for the Excess Gibbs Free Energy of Liquid Mixtures. *Fluid Phase Equilib.* **1977**, *1*, 113.
(24) Prausnitz, J. M.; Lichtenthaler, R. N.; Gomes de Azevedo, E. *Molecular Thermodynamics of Fluid-Phase Equilibria*, 3rd ed.; Prentice Hall: Upper Saddle River, NJ, 1999.
(25) Peng, D.-Y. Extending the van Laar Model to Multicomponent Systems. *Open Thermodyn. J.* **2010**, *4*, 129.
(26) Karásek, P.; Planeta, J.; Roth, M. Simple First-Order Group Contribution Scheme for Solubilities of Solid Polycyclic Aromatic Hydrocarbons and Solid Polycyclic Aromatic Heterocycles in Pressurized Hot Water. *Ind. Eng. Chem. Res.* **2008**, *47*, 620.
(27) Hurst, J. E., Jr.; Harrison, B. K. Estimation of Liquid and Solid Heat Capacities using a Modified Kopp's Rule. *Chem. Eng. Commun.* **1992**, *112*, 21.
(28) Shah, P. N.; Yaws, C. L. Densities of Liquids. *Chem. Eng.* **1976**, *83*, 131.
(29) Valderrama, J. O.; Sanga, W. W.; Lazzús, J. A. Critical Properties, Normal Boiling Temperature, and Acentric Factor of Another 200 Ionic Liquids. *Ind. Eng. Chem. Res.* **2008**, *47*, 1318.
(30) Alvarez, V. H.; Valderrama, J. O. Metodo Modificado Lydersen-Joback-Reid para Estimar las Propriedades Criticas de Biomoleculas. *Alimentaria* **2004**, *354*, 55.
(31) Goodman, B. T.; Wilding, W. V.; Oscarson, J. L.; Rowley, R. L. A Note on the Relationship between Organic Solid Density and Liquid Density at the Triple Point. *J. Chem. Eng. Data* **2004**, *49*, 1512.
(32) Alvarez, V. H.; Larico, R.; Yanos, Y.; Aznar, M. Parameter Estimation for VLE Calculation by Global Minimization: Genetic Algorithm. *Braz. J. Chem. Eng.* **2008**, *25*, 409.
(33) Diadem Public 1.2. The DIPPR Information and Data Evaluation Manager; 2000.
(34) Molecular Modeling Pro, demo version; http://www.chemsw.com (accessed Dec 1, 2010).
(35) Bosque, R.; Sales, J. Polarizabilities of Solvents from the Chemical Composition. *J. Chem. Inf. Comput. Sci.* **2002**, *42*, 1154.
(36) Rasmussen, P. Developments in G^E Models Including Group Contributions. *Fluid Phase Equilib.* **1983**, *13*, 213.
(37) Karásek, P.; Planeta, J.; Roth, M. Aqueous Solubility Data for Pressurized Hot Water Extraction for Solid Heterocyclic Analogs of Anthracene, Phenanthrene and Fluorene. *J. Chromatogr., A* **2007**, *1140*, 195.
(38) Andersson, T. A.; Hartonen, K. M.; Riekkola, M.-L. Solubility of Acenaphthene, Anthracene, and Pyrene in Water at 50 to 300 °C. *J. Chem. Eng. Data* **2005**, *50*, 1177.